Biosensors and Bioelectronics 57 (2014) 71–76

Contents lists available at ScienceDirect

Biosensors and Bioelectronics

journal homepage: www.elsevier.com/locate/bios

Bi-pseudoenzyme synergetic catalysis to generate a coreactant of peroxydisulfate for an ultrasensitive electrochemiluminescence-based cholesterol biosensor

Juanjuan Zhang, Wanting Wang, Shihong Chen*, Yuan Ruo*, Xia Zhong, Xiaoping Wu

Education Ministry Key Laboratory on Luminescence and Real-Time Analysis, College of Chemistry and Chemical Engineering, Southwest University, Chongqing 400715, China

ARTICLE INFO

Article history:
Received 6 December 2013
Received in revised form
22 January 2014
Accepted 23 January 2014
Available online 3 February 2014

Keywords:
Electrochemiluminescence
Peroxydisulfate
Graphene
Hemin
Cholesterol
Biosensor

ABSTRACT

A novel electrochemiluminescence (ECL) enzyme biosensor for the ultrasensitive detection of cholesterol was designed based on a bi-pseudoenzymatic reaction to generate a coreactant of peroxydisulfate for signal amplification. In this work, hemin-functionalized graphene (hemin-GR) was synthesized and used to immobilize cholesterol oxidase (COx) to construct an ECL biosensor for cholesterol. When cholesterol was added to the detection solution, COx catalyzed the oxidation of cholesterol to generate H_2O_2, which could be further catalyzed by hemin to produce O_2 as the coreactant in the peroxydisulfate system for signal amplification. The linear range for cholesterol detection was 3.3–1,500 nM, with a lower detection limit of 1.0 nM (signal to noise ratio=3). Therefore, the detection limit and sensitivity of the biosensor were improved. This novel strategy offers advantages of simplicity, improved sensitivity, good selectivity, and repeatability, and therefore, holds promise for use in sensitive bioassays for clinical determination of cholesterol levels.

© 2014 Elsevier B.V. All rights reserved.

1. Introduction

As a chemical detection method, electrochemiluminescence (ECL) is steadily becoming an important and powerful analytical tool in the fields of environmental pollutant determination, pharmaceutical analysis, and immunoassay due to its advantages of simplicity, rapidity, sensitivity, controllability, and low background noise (Bertoncello and Forster, 2009; Miao, 2008; Zhou et al., 2003). ECL regents such as luminol species, peroxydisulfate, Ru complex, and quantum dots have been widely applied to construct ECL immunosensors and DNA and RNA biosensors (Egashira et al., 2008; Jie et al., 2007; Li and Cui, 2013; Tian et al., 2009; Wang et al., 2012a,b; Zhan and Bard, 2007). Specifically, ECL based on luminol species was recently applied in enzyme biosensors for glucose and cholesterol. These enzyme biosensors demonstrated high sensitivity and low detection limits (Ballesta-Clavera et al., 2012; Rad et al., 2012; Zhang et al., 2012). However, random peaks that could not be attributed to luminol usually appeared. Furthermore, the sensitivity and detection limit could be further improved.

Peroxydisulfate ($S_2O_8^{2-}$) solution represents a novel ECL system that can be used in enzymatic assays. The ECL mechanism of the peroxydisulfate system is as follows (Reshetnyak and Koval'chuk, 1998; Yao et al., 2008):

$$S_2O_8^{2-} + e \rightarrow SO_4^{\bullet -} + SO_4^{2-}$$

$$SO_4^{\bullet -} + H_2O \rightarrow HO^{\bullet} + HSO_4^{-}$$

$$HO^{\bullet} \rightarrow HOO^{\bullet} + H_2O$$

$$O_2 + H_2O + e \rightarrow HOO^{\bullet} + HO^{-}$$

$$SO_4^{\bullet -} + HOO^{\bullet} \rightarrow HSO_4^{-} + {}^1(O_2)_2^*$$

$${}^1(O_2)_2^* \rightarrow 2\,{}^3O_2 + h\nu$$

Herein, oxygen (O_2) serves as the coreactant in the peroxydisulfate system, and the ECL intensity increases with O_2 saturation of the solution (Reshetnyak and Koval'chuk, 1998). This is the basis of the quantitative analysis in our experiment. The peroxydisulfate-based ECL system is a promising option for enzyme biosensors that achieve quantitative analysis of biologically active substances, because many biologically active substances (e.g., glucose, cholesterol, lactate, choline, and others) can be metabolized or transformed into H_2O_2 by the catalytic action of enzymes (Ram et al., 2001; Wang and Zhang, 2013; Yu et al., 2013) and H_2O_2 is further transformed or metabolized to O_2 with the help of peroxidase or mimicry of peroxidase (Freeman et al., 2011), which leads to a change in ECL intensity. To the best of our knowledge, no progress

* Corresponding authors. Tel./fax: +86 23 68 25 3172.
E-mail addresses: cshong@swu.edu.cn (S. Chen), yuanruo@swu.edu.cn (Y. Ruo).

0956-5663/$ - see front matter © 2014 Elsevier B.V. All rights reserved.
http://dx.doi.org/10.1016/j.bios.2014.01.046

has been made in constructing a peroxydisulfate-based ECL enzyme biosensor until now.

As a well-known natural porphyry-inatoiron, hemin (iron proporphyrin IX) is often used to mimic peroxidase (Wang et al., 1999; Zhang and Dasgupta, 1992). Furthermore, it can be adsorbed onto the surface of graphene through π–π stacking and hydrophobic interactions to form a hemin-graphene nanocomposite (hemin-GR). This composite not only serves to mimic peroxidase but also possesses the beneficial properties of graphene such as large surface area, high conductivity, and great mechanical strength. Therefore, the hemin-GR nanocomposite offers excellent potential for applications in the fields of electrocatalysis, artifical enzyme mimetics, biosensors, and luminescence (Guo et al., 2011).

Motivated by the above observations, in the present work, we used hydrazine to reduce graphene oxide in the presence of poly (diallydimethylammonium chloride) (PDDA). Herein, hydrazine acted as the reducing agent, and positively charged PDDA served as the stabilizer to prevent aggregation of the reduced graphene. Subsequently, hemin was absorbed onto graphene under sonication to form hemin-GR. Then, the positively charged hemin-GR nanocomposite was modified on the surface of a glassy carbon electrode to adsorb negatively charged cholesterol oxidase (COx, the model enzyme) through electrostatic interaction. This proposed biosensor exhibited a low detection limit for cholesterol due to the high sensitivity of the peroxydisulfate ECL system. Therefore, ECL employing the peroxydisulfate solution system offers a promising means for improving the sensitivity of enzyme biosensors.

2. Experimental

2.1. Reagents

Cholesterol oxidase (COx, EC 1.1.3.6 from *Brevibacterium* sp., ≥ 50 units/mg), cholesterol, iron proporphyrin, and Triton X-100 were all purchased from Sigma Chemical Co. (St. Louis, MO, USA). Graphene oxide (GO) was purchased from Nanking Xianfeng Nano Co. (Nanking, China). PDDA was obtained from Beiking Chemical Reagent Co. (Beking, China). Phosphate-buffered saline (PBS) solutions containing 0.9% NaCl with pH 7.0 were prepared with 0.10 M H_3PO_4, adjusted pH with concentrated NaOH solution. A stock cholesterol solution (1.0 mM) was prepared in PBS (0.10 M, pH 7.0) containing 10% (w/w) Triton X-100 in a heated water bath at 65 °C and then stored at 4 °C. All other chemicals were of analytical grade and were used as received. Deionized water was used throughout this study.

2.2. Apparatus

ECL emission was measured using a model MPI-A electrochemiluminescence analyzer (Xi'an Remax Electronic Science & Technology Co. Ltd., China), equipped with a photomultiplier tube (PMT) with the voltage set at 800 V for detection. Cyclic voltammetry (CV) was carried out with a CHI 600D electrochemical work station (Shanghai CH Instruments Co., China). Absorption spectra were recorded by a UV-2450 UV–vis spectrophotometer from the Shimadzu Corp. (Japan). The conventional three-electrode system, including a modified glassy carbon electrode (GCE) as the working electrode, a saturated calomel electrode (SCE) or Ag/AgCl (saturated KCl) as reference electrodes, and a platinum wire as counter electrode was used in the detection process. Scanning electron microscopy (SEM) was conducted using a Hitachi scanning electron microscope (Hitachi, S-4800, Japan). The topographs of films modified with different materials were investigated with atomic force microscopy (AFM, dimension ICON, USA). All of the above experiments were carried out at room temperature.

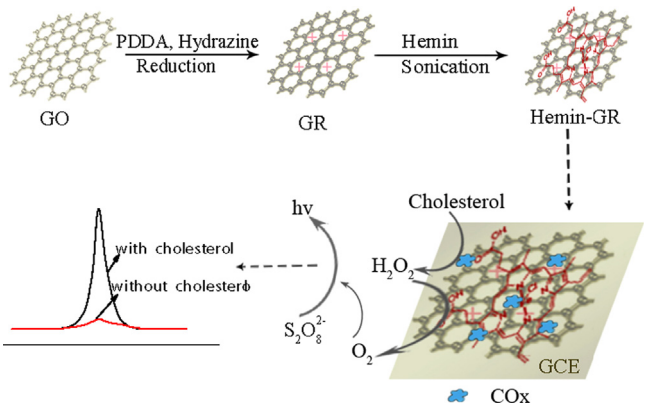

Scheme 1. Schematic representation of the procedure for preparing hemin-GR nanocomposite and the bi-pseudoenzyme synergetic catalysis mechanism based on COx and hemin for signal amplification.

2.3. Synthesis of hemin-GR nanocomposite

First, reduced graphene (GR) was synthesized according to a previously described method (Bai et al., 2012) with some modification. Briefly, 0.030 mL PDDA (20%) was added to 10 mL graphene oxide suspension (0.50 mg/mL) and then stirred for 30 min. Then, 50 μL hydrazine hydrates (80%) was added and heated with stirring in a water bath (90 °C) for approximately 12 h. The obtained black reduced graphene was washed three times by centrifugation with double distilled water and then redispersed in water. Second, hemin-functionalized graphene (hemin-GR) was synthesized as follows. Hemin (5.0 mg) was added to the previous reduced graphene dispersion and sonicated for 4 h at room temperature. The reactant was then washed by centrifugation and redispersed in water. The corresponding synthesis process is shown in Scheme 1.

2.4. Biosensor preparation

The glassy carbon electrode (GCE, Φ=4 mm) was carefully polished with 0.3 μm and 0.05 μm alumina and then ultrasonically washed with ethanol and water for 3 min each. Next, 5 μL hemin-GR suspension was cast onto a pretreated GCE surface and dried at room temperature. Subsequently, 5 μL COx solution was dropped onto the electrode to achieve the biosensor COx/hemin-GR/GCE. This fabrication procedure is schematically presented in Scheme 1. The biosensor was stored at 4 °C in a refrigerator when not in use.

3. Results and discussion

3.1. Characterization of the nanocomposite

Fig. 1 presents the UV–vis absorption spectra of GR and hemin-GR nanocomposite dispersed in water. In the UV–visible spectrum of GR (curve a), the peak at 270 nm was attributed to the $\pi \rightarrow \pi^*$ transition of C=C of GR (Li et al., 2011). This peak red-shifted to 275 nm after hemin was conjugated to GR (curve b). Another peak at 420 nm was observed on curve *b* and could be attributed to hemin. Compared to the previous results (Guo et al., 2011), the peaks of both GR and hemin were red-shifted by approximately several nanometers, which can be attributed to the effect of PDDA.

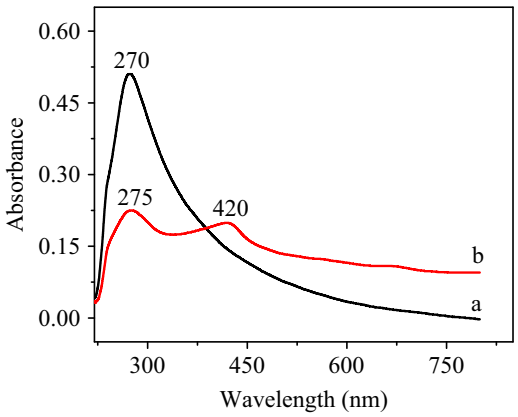

Fig. 1. UV–visible spectra of (a) GR and (b) hemin-GR nanocomposite.

3.2. Characterization of the biosensor fabrication process

SEM was employed to characterize the biosensor fabrication process. Typical SEM images of different modified films are shown in Fig. 2. As seen in Fig. 2(A), hemin-GR exhibited a typical wrinkle morphology and paper-like shape with very thin layers. After COx was adsorbed onto the surface of hemin-GR (Fig. 2(B)), as expected, the surface of the resulting COx/hemin-GR film became blurry and smooth due to coverage with COx.

AFM was conducted to observe the surface topographies of the hemin-GR and COx/hemin-GR. Fig. 2(C) shows an AFM image of the hemin-GR film modified on the mica substrate. A flake-like nanostructure was clearly observed. The corresponding cross-sectional view is shown in Fig. 2(E) and the average thickness of hemin-GR was about 1–2 nm, which is a typical characteristic of functional molecule-protected single-layer graphene (Rao et al., 2009). After COx was modified, the surface of hemin-GR became "lighter", as shown in Fig. 2(D). This was because the absorbed enzyme molecules increased the thickness of the modified film. Fig. 2(F) shows a cross-sectional view of Fig. 2(D), and the average thickness of the modified film of ~13 nm was estimated from Fig. 2(F) and is consistent with values presented in previous reports (Ram et al., 2001).

CV was also used to probe the interfacial characteristics of the electrodes. Fig. S1 shows the cyclic voltammograms of the different modified electrodes in 5.0 mM $[Fe(CN)_6]^{4-/3-}$ solution. Well-defined oxidation and reduction peaks of $[Fe(CN)_6]^{4-/3-}$ were observed at the bare GCE (Fig. S1 (curve a)). After the hemin-GR nanocomposite was modified on the surface of GCE (Fig. S1 (curve b)), a decrease in the peak current was noticed due to the insulating property of hemin and PDDA, indicating that the hemin-GR nanocomposite had been immobilized successfully. When COx was cast onto the electrode (Fig. S1 (curve c)), the peak current further decreased because of the hindrance of non-conductive COx.

Furthermore, electrochemical impedance spectroscopy (EIS) is a useful tool for evaluating the interfacial changes of an electrode. The semicircle diameter of impedance equals the electron transfer resistance (R_{et}), which controls the electron transfer kinetics of the redox probe at the electrode interface. Fig. 3(A) presents the impedance spectrum of each modified stage. Compared with the bare GCE (Fig. 3(A) (curve a)), the Nyquist semicircle of hemin-GR/GC (Fig. 3(A) (curve b)) in 5.0 mM $K_3Fe(CN)_6/K_4Fe(CN)_6$ (1:1) was increased, which indicates that hemin-GR was immobilized on the GCE. After the COx was immobilized onto the electrode, the Nyquist semicircle further increased (Fig. 3(A) (curve c)) due to hindrance caused by non-conductive COx.

The ECL behavior of the fabricated biosensor was investigated. Fig. 3(B) shows the ECL signals at different modified electrodes in 0.10 M PBS, pH 7.0, containing 0.10 M $S_2O_8^{2-}$. Compared to the bare GCE (Fig. 3(B) (curve a)), the ECL intensity at the hemin-GR/GCE decreased (Fig. 3(B) (curve b)). After COx was immobilized on the electrode (Fig. 3(B) (curve c)), the ECL intensity further decreased. The ECL behavior was consistent with that determined by CV and EIS. To confirm the role of $S_2O_8^{2-}$ in this ECL system, the ECL responses were investigated for the proposed biosensor (COx/hemin-GR/GCE) in different detection solutions. Fig. S2(A) displays the ECL responses of COx/hemin-GR/GCE without (curve a) and with 1,500 nM (curve b) cholesterol in 0.10 M blank PBS. As seen, no obvious ECL signal was observed. Fig. S2(B) shows the ECL responses of COx/hemin-GR/GCE in 0.10 M PBS containing 0.34 mM H_2O_2. In this case, we could also not observe the ECL signal before (Fig. S2(B) (curve a)) and after (Fig. S2(B) (curve b)) adding 1,500 nM cholesterol in detection solution. However, when the detection solution contained 0.10 M $S_2O_8^{2-}$, an ECL signal was observed at COx/hemin-GR/GCE even in the absence of cholesterol (Fig. S2(C) (curve a)). The intensity of this ECL signal increased with the addition of 1,500 nM cholesterol (Fig. S2(C) (curve b)). This increase was attributed to H_2O_2, which was generated by the catalytic action of COx and further transformed or metabolized to O_2 with the help of hemin. Herein, O_2 served as the coreactant in the peroxydisulfate ECL system for signal amplification, thus leading to an increase in the ECL intensity. The results of above control experiments demonstrated that the detection of cholesterol could not be achieved in the case only with H_2O_2 but without $S_2O_8^{2-}$ in PBS, and only when $S_2O_8^{2-}$ was presented in the detection solution could the ECL signal be observed and enhanced by cholesterol.

3.3. Optimization of the $S_2O_8^{2-}$ concentration

The effect of the concentration of $S_2O_8^{2-}$ on the ECL signal was investigated, and the corresponding results are shown in Fig. S3. The intensity of the ECL signal distinctly increased as the concentration of $S_2O_8^{2-}$ increased in the range of 0.030–0.10 M. After the concentration of $S_2O_8^{2-}$ was increased to 0.10 M, only a slight increase in the ECL signal was observed. Thus, 0.10 M $S_2O_8^{2-}$ was used in further experiments.

3.4. Quantitative analysis of cholesterol at the COx/hemin-GR/GCE

A quantitative analysis of cholesterol was conducted at the COx/hemin-GR/GCE in 0.10 M $S_2O_8^{2-}$ solution. As shown in Fig. 4(A), when cholesterol was added into the analytical cell, an increase in the ECL signal intensity was observed. The ECL intensity was linear with the cholesterol concentration from 3.3–1,500 nM, as presented in the inset of Fig. 4(A). After the concentration was increased to 3,500 nM, only a slight increase in the ECL signal was observed. Higher cholesterol levels could be detected by appropriate dilution with PBS. The corresponding calibration equation was I (a.u.) = 175.0 + 1.520c (nM), with a correlation coefficient R^2 0.994. From the slope of calibration curve, a detection limit of 1.0 nM is estimated at a signal-to-noise ratio of 3. This detection limit was about 1000 times lower than previously reported values (Zhang et al., 2012; Ballesta-Clavera et al., 2012; Zhang et al., 2013). Also, the sensitivity (estimated by the slope of the calibration curve) was improved compared with the results of recent reports based on a luminol-ECL system (Zhang et al., 2012; Ballesta-Clavera et al., 2012; Zhang et al., 2013). The details of a comparison between our method and their methods are provided in Table 1. Overall, the proposed biosensors in this work exhibited excellent performance due to the synergetic effects of each component in a hemin-GR nanocomposite and the high sensitivity of the peroxydisulfate ECL system.

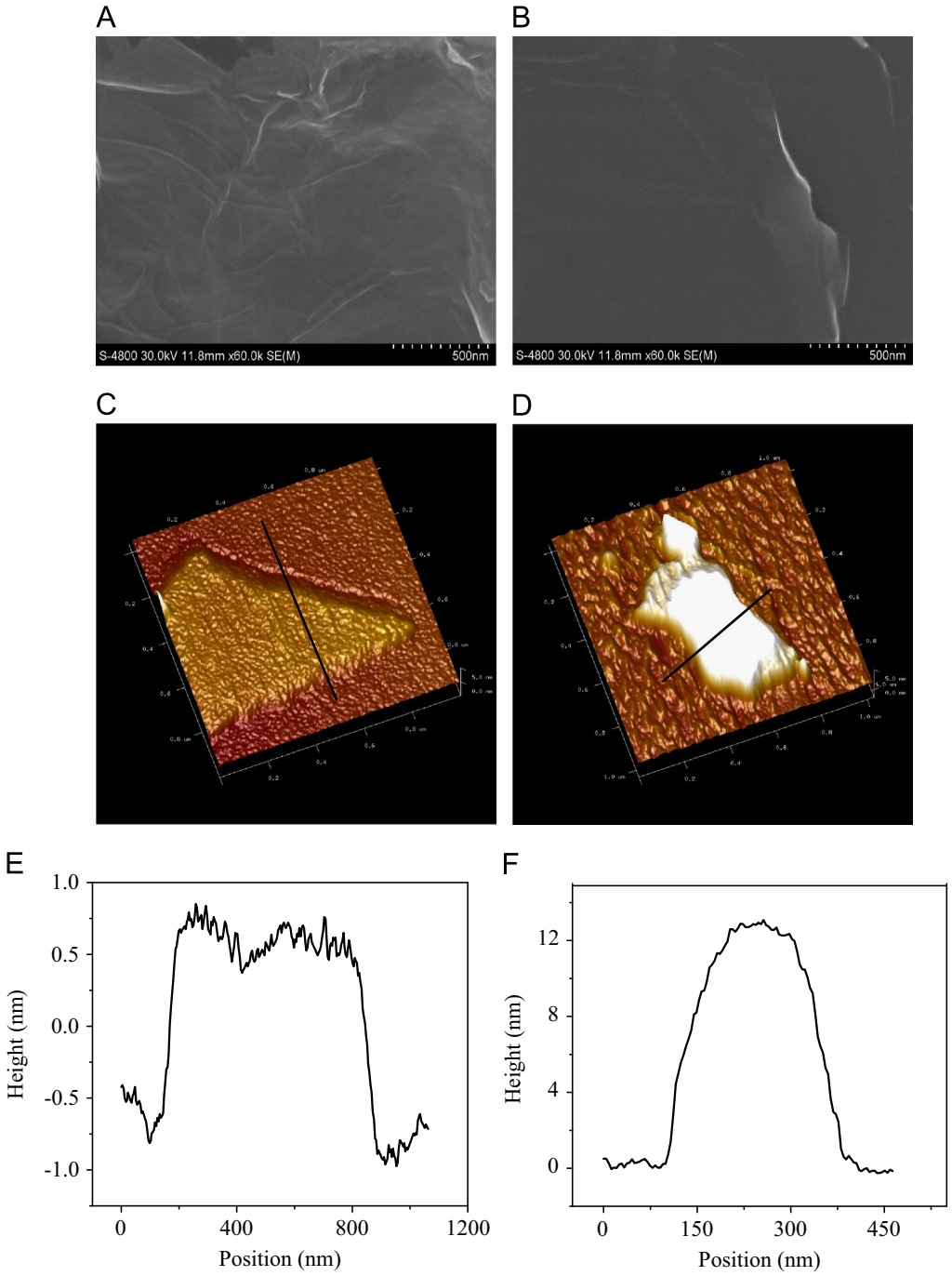

Fig. 2. SEM images of (A) hemin-GR and (B) COx/hemin-GR modified film. AFM images of (C) hemin-GR and (D) COx/hemin-GR modified film. (E) and (F) Cross-sectional views along the lines in (C) and (D), respectively.

3.5. *Repeatability, stability, and specificity of ECL cholesterol biosensor*

Repeatability, stability, and specificity are important factors for evaluating the performance of biosensors. The repeatability was studied by continuously cyclic potential scanning for 14 cycles in detection solution containing 1.0 μM cholesterol, and the results are shown in Fig. 4(B). A relative standard deviation (RSD) of 4.4% was achieved. The long-term stability of the biosensor was investigated by ECL measurement. The ECL response decreased to 91.6% after 1 week. To investigate the specificity of our proposed biosensors, some biomolecules that coexist with cholesterol in serum such as dopamine, uric acid, ascorbic acid, and glucose were used as sources of interference. As expected, 5.0 μM of these substances did not result in a noticeable ECL signal change for the detection of 1.0 μM cholesterol. Our experimental results demonstrated good repeatability, stability, and specificity of the proposed biosensors.

3.6. *Application of the biosensors*

The analytical reliability and potential application of the biosensors were investigated via a standard addition method. Standard cholesterol solutions of different concentrations were individually added into diluted normal human serum samples. The corresponding results are shown in Table 1S. The recoveries and the relative standard derivations of the proposed cholesterol biosensors were in the range of 97.3–110%

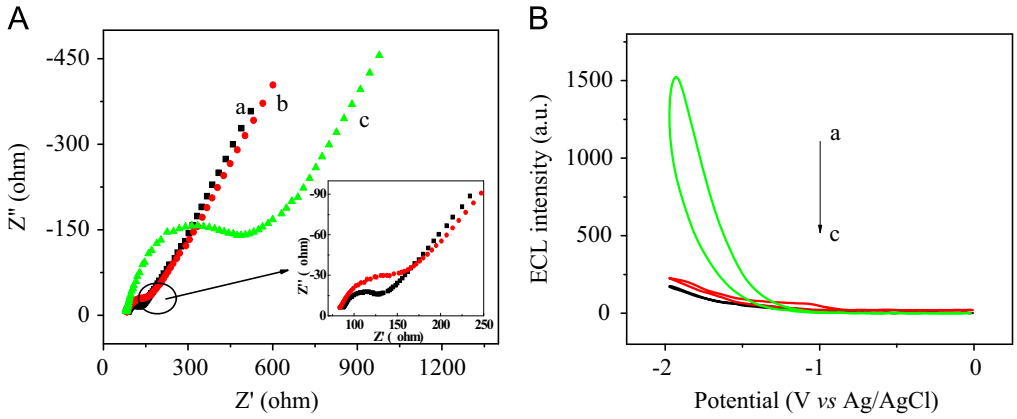

Fig. 3. (A) EIS of (a) bare GCE, (b) hemin-GR/GCE, and (c) COx/hemin-GR/GCE in 5.0 mM $K_3[Fe(CN)_6]/K_4[Fe(CN)_6]$ (1:1). Scan rate: 50 mV/s. (B) ECL behavior of (a) bare GCE, (b) hemin-GR/GCE, and (c) COx/hemin-GR/GCE in 0.10 M, pH 7.0, PBS containing 0.10 M $S_2O_8^{2-}$.

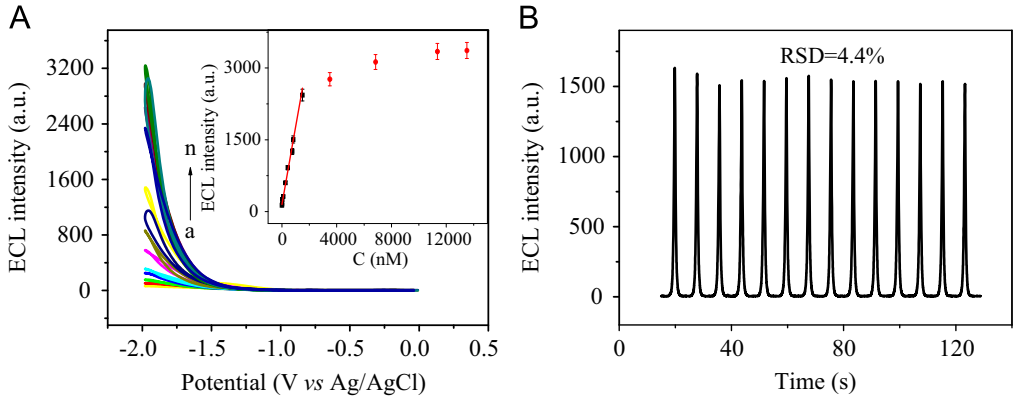

Fig. 4. (A) ECL responses of COx/hemin-GR/GCE to (a) 0, (b) 3.3, (c) 13.3, (d) 33.3, (e) 100, (f) 266.7, (g) 433.3, (h) 766.6, (i) 833.3, (j) 1,500, (k) 3,500, (l) 6,833.3, (m) 11,350 and (n) 13,500 nM cholesterol in 0.10 M PBS (pH 7.0) containing 0.10 M $S_2O_8^{2-}$. Inset shows the linear relationship between the ECL signal intensity and the concentration of cholesterol. (B) The stability of the biosensor under consecutive cyclic potential scans for 14 cycles in 1.0 μM cholesterol solution. Scan rate: 0.50 V/s.

Table 1
Comparison of different methods for the determination of cholesterol.

Materials	Method	Linear range	Slope	Detection limit	Reference
l-cys-rGO composites	Luminol-ECL	$(3.3–1000)\times10^{-6}$ M	1.53×10^{4} a.u./mM	1.1 μM	Zhang et al., 2012
CeO_2-graphene	Luminol-ECL	$(12–7200)\times10^{-6}$ M	1.29×10^{4} a.u./mM	4.0 μM	Zhang et al., 2013
poly(luminol-biotinylated pyrrole)	Luminol-ECL	1.5×10^{-5}–8.0×10^{-4} M	–	14.7 μM	Ballesta-Clavera et al., 2012
TiO_2–graphene–Pt–Pd	Amperometry	5.0×10^{-8}–5.9×10^{-4} M	–	0.017 μM	Cao et al., 2013
AuPt–Ch–IL	Amperometry	0.05–6.2 mM and 6.2–11.2 mM.	–	–	Safavia and Farjami, 2011
Hemin-GR	$S_2O_8^{2-}$-ECL	3.3–1,500 nM	1.52×10^{6} a.u./mM	1.0 nM	This work

and 2.3–7.3% ($n=3$), respectively, indicating an acceptable accuracy for analytical application to human serum samples.

4. Conclusion

A novel strategy for constructing an ECL enzyme biosensor based on the peroxydisulfate system was proposed. Namely, a bi-pseudoenzymatic reaction was designed to generate O_2 as the coreactant of the peroxydisulfate system for signal amplification. The nanocomposite hemin-GR was synthesized to immobilize cholesterol oxidase. Herein, hemin acted as a mimic of peroxidase to construct a bi-pseudoenzyme system. Graphene as the substrate of hemin can improve the ECL signal and enhance the detection sensitivity. Positively charged PDDA is able to immobilize the more negatively charged COx. Due to the synergetic effects of each component in the hemin-GR nanocomposite and the high sensitivity of the peroxydisulfate ECL system, the proposed biosensors exhibited high sensitivity, good repeatability, and acceptable stability and accuracy. Thus, this work provided a new method for constructing an ECL enzyme biosensor, which will extend the application of an ECL detection method in enzymatic assays.

Acknowledgments

This work was supported by the National Natural Science Foundation of China (21075100 and 21275119), the Ministry of Education of China (708073), Specialized Research Fund for the Doctoral Program of Higher Education (20100182110015), the State Key Laboratory of Electroanalytical Chemistry (SKLEAC 2010009), the Natural Science Foundation Project of Chongqing City

(CSTC-2011BA7003), and the Fundamental Research Funds for the Central Universities (XDJK2012A004).

Appendix A. Supporting information

Supplementary data associated with this article can be found in the online version at http://dx.doi.org/10.1016/j.bios.2014.01.046.

References

Bai, L.J., Yuan, R., Chai, Y.Q., Yuan, Y.L., Wang, Y., Xie, S.B., 2012. Chem. Commun. 48, 10972–10974.
Ballesta-Clavera, J., Ametis-Cabelloa, J., Morales-Sanfrutosb, J., Megía-Fernándezb, A., Valencia-Miróna, M.C., Santoyo-Gonzálezb, F., Capitán-Vallveya, L.F., 2012. Anal. Chim. Acta 754, 91–98.
Bertoncello, P., Forster, R.J., 2009. Biosens. Bioelectron. 24, 3191–3200.
Cao, S.R., Zhang, L., Chai, Y.Q., Yuan, R., 2013. Biosens. Bioelectron. 42, 532–538.
Egashira, N., Morita, S.I., Hifumi, E., Mitoma, Y., Uda, T., 2008. Anal. Chem. 80, 4020–4025.
Freeman, R., Liu, X.Q., Willner, I., 2011. J. Am. Chem. Soc. 133, 11597–11604.
Guo, Y.J., Deng, L., Li, J., Guo, S.J., Wang, E.K., Dong, S.J., 2011. ACS Nano 5, 1282–1290.
Jie, G.F., Liu, B., Pan, H.C., Zhu, J.J., Chen, H.Y., 2007. Anal. Chem. 79, 5574–5581.
Li, F., Cui, H., 2013. Biosens. Bioelectron. 39, 261–267.
Li, L.L., Liu, K.P., Yang, G.H., Wang, C.M., Zhang, J.R., Zhu, J.J., 2011. Adv. Funct. Mater. 21, 869–878.
Miao, W., 2008. Chem. Rev. 108, 2506–2553.
Rad, A.S., Ardjmand, M., Jahanshahi, M., Safekordi, A., 2012. Korean J. Chem. Eng. 29, 1063–1068.
Ram, M.K., Bertoncello, P., Ding, H., Paddeu, S., Nicolini, C., 2001. Biosens. Bioelectron. 16, 849–856.
Rao, C.N.R., Sood, A.K., Subrahmanyam, K.S., Govindaraj, A., 2009. Angew. Chem. Int. Ed. 48, 7752–7777.
Reshetnyak, O.V., Koval'chuk, E.P., 1998. Electrochim. Acta 43, 465–469.
Safavia, A., Farjami, F., 2011. Biosens. Bioelectron. 26, 2547–2552.
Tian, D.Y., Duan, C.F., Wang, W., Li, N., Zhang, H., Cui, H., Lu, Y.Y., 2009. Talanta 78, 399–404.
Wang, H.J., Yuan, R., Chai, Y.Q., Niu, H., Cao, Y.L., Liu, H.J., 2012a. Biosens. Bioelectron. 37, 6–10.
Wang, J., Han, H., Jiang, X.C., Huang, L., Chen, L., Li, N., 2012b. Anal. Chem. 84, 4893–4899.
Wang, X.L., Zhang, X.L., 2013. Electrochim. Acta 112, 774–782.
Wang, X.Q., Li, Y.Z., Chang, W.B., 1999. Anal. Chim. Acta 400, 135–142.
Yao, W., Wang, L., Wang, H.Y., Zhang, X.L., 2008. Electrochim. Acta 54, 733–737.
Yu, Y.Y., Yang, Y., Gu, H., Zhou, T.S., Shi, G.Y., 2013. Biosens. Bioelectron. 41, 511–518.
Zhan, W., Bard, A.J., 2007. Anal. Chem. 79, 459–463.
Zhang, G., Dasgupta, P., 1992. Anal. Chem. 64, 517–522.
Zhang, M.H., Yuan, R., Chai, Y.Q., Chen, S.H., Zhong, H.A., Wang, C., Cheng, Y.F., 2012. Biosens. Bioelectron. 32, 288–292.
Zhang, M.H., Yuan, R., Chai, Y.Q., Wang, C., Wu, X.P., 2013. Anal. Biochem. 436, 69–74.
Zhou, M., Roovers, J., Robertson, G.P., Grover, C.P., 2003. Anal. Chem. 75, 6708–6717.